Developmental Biology **233,** 482–494 (2001)
doi:10.1006/dbio.2001.0235, available online at http://www.idealibrary.com on IDEAL®

Early Morphogenesis of the *Caenorhabditis elegans* Pharynx

Michael F. Portereiko and Susan E. Mango[1]

Department of Oncological Sciences and Huntsman Cancer Institute Center for Children, University of Utah, 2000 Circle of Hope, Salt Lake City, Utah 84112

We investigated the cellular behaviors that accompany the early stages of pharyngeal morphogenesis in *Caenorhabditis elegans*. The embryonic pharynx develops from a ball of cells into a linear tube connected anteriorly to the buccal cavity and posteriorly to the midgut. By using GFP reporters localized to discrete subcellular regions, we show that pharyngeal morphogenesis can be divided into three stages: (1) lengthening of the nascent pharyngeal lumen by reorientation of apicobasal polarity of anterior pharyngeal cells ("Reorientation"), (2) formation of an epithelium by the buccal cavity cells, which mechanically couples the buccal cavity to the pharynx and anterior epidermis ("Epithelialization"), and (3) a concomitant movement of the pharynx anteriorly and the epidermis of the mouth posteriorly to bring the pharynx, buccal cavity, and mouth into close apposition ("Contraction"). Several models can account for these cellular behaviors, and we distinguish between them by physically or genetically ablating cells within the digestive tract. These studies provide the first description of how the pharynx primordium develops into an epithelial tube, and reveal that pharyngeal morphogenesis resembles aspects of mammalian kidney tubulogenesis.

Key Words: **morphogenesis; tubulogenesis; embryogenesis; foregut; pharyngeal extension; epithelia.**

INTRODUCTION

The precise regulation of cell movement and shape plays a key role in generating the three-dimensional architecture of tissues and organs. Tubes, which are used to transport fluids, food, or air throughout the body, are a common component of many organs. Studies with a diverse array of organs and animals have shown that tubes arise either from sculpting preexisting epithelia into tubular structures (e.g., lung, trachea; Metzger and Krasnow, 1999) or from coalescing mesenchymal cells to generate tubular epithelia *de novo* (e.g., kidney; Kuure *et al.*, 2000). These events are under control of a complex network of signaling pathways, transcription factors, and adhesion molecules (Hogan, 1999; Metzger and Krasnow, 1999; Kuure *et al.*, 2000).

Caenorhabditis elegans provides a powerful system to study morphogenetic events including tube formation (this study, and Leung *et al.*, 1999), cell migration (Chen and Stern, 1998; Montell, 1999), and epidermal epiboly (Priess and Hirsh, 1986; Williams-Masson *et al.*, 1997; George *et al.*, 1998; Williams-Masson *et al.*, 1998; Raich *et al.*, 1999; Roy *et al.*, 2000; reviewed in Chin-Sang and Chisholm, 2000; Simske and Hardin, 2001). Cellular behavior can be followed at the resolution of single cells and in living animals; the molecular components that guide these behaviors can be identified by forward and reverse genetics. Here, we investigate pharynx morphogenesis as an example of tube formation in *C. elegans*. While numerous studies have contributed to our understanding of cell fate specification of pharyngeal cells (Schnabel and Priess, 1997; Labouesse and Mango, 1999), the mechanisms that drive pharyngeal morphogenesis have not been examined.

The pharynx represents the foregut of the nematode digestive tract. The mature digestive tract is organized as a linear epithelial tube that is regionalized both spatially and functionally (White, 1988; Avery and Thomas, 1997). Food (bacteria) is pumped in through the buccal cavity by the action of the muscular pharynx, "chewed" by specialized cuticle lining the pharynx, and passed on to the midgut for the bulk of digestion; wastes are expelled through the rectum and anus (or nematode hindgut). The digestive tract provides a simple example of a linear gut since it has few cells (127) and no organ outpocketings. Much of the digestive tract is organized as a series of rings composed of two or three cells arranged with bi- or trilateral symmetry. The

[1] To whom correspondence should be addressed. E-mail: susan.mango@hci.utah.edu.

0012-1606/01 $35.00

pharynx is more complex, with eight sets of cells joined end to end by adherens junctions. Most of these sets are composed of six cells (six to nine nuclei) arranged with threefold rotational symmetry around a Y-shaped lumen (Albertson and Thomson, 1976).

The pharynx undergoes dramatic shape changes during development, from a ball to a tube. By midembryogenesis, gastrulation is complete and the pharyngeal primordium is visible as a ball of cells bordering the nascent midgut in the interior of the embryo (Sulston *et al.*, 1983). The pharyngeal cells are attached to each other and to the midgut by adherens junctions (Leung *et al.*, 1999), but are not yet connected to the buccal cavity. Over the next 60 min, the pharyngeal cells shift their position and organization to form a linear tube that links the digestive tract to the exterior. We call this process "pharyngeal extension." During later embryogenesis, this tube develops a lumen and undergoes a complicated program of differentiation and morphogenesis to produce the characteristic bilobed structure of the mature pharynx. Because cell division is largely complete at this stage, pharyngeal extension is driven by forces other than cell proliferation (Sulston *et al.*, 1983).

We have used a combination of Nomarski differential interference contrast (DIC) and fluorescence imaging to study pharyngeal extension. By targeting green fluorescent protein (GFP) to different subcellular locations, we have been able to follow the shape and position of individual pharyngeal and buccal cavity cells in living embryos. Our data reveal that cell movements such as cell migration or cell intercalation, which are frequently involved in other morphogenetic processes, do not appear to play a significant role here. Rather, pharyngeal extension depends on the coordinate formation of new epithelia to link cells of the pharynx with those of the buccal cavity and epidermis. Once these cells become attached to one another, we propose that a local contraction provides the force that pulls these cells together and constricts their apical surfaces. These behaviors produce the characteristic teardrop morphology of the nascent pharynx at midembryogenesis.

MATERIALS AND METHODS

Nematode Strains and Culture

The JAM-1::GFP strain *jcIs1* expresses GFP in adherens junctions and is a marker of epithelialization (Mohler *et al.*, 1998). *C. elegans* strains were cultured as described previously (Brenner, 1974). JJ1057 (*pop-1(zu189) dpy-5(e61)/hT1* I; *him-5(e1490)/hT1* V; Lin *et al.*, 1995) was used for *pop-1* mutant analyses.

Plasmids

For **GFP-N**, GFP from pPD 103.87 (http://www.ciwemb.edu; Fire *et al.*, 1990) was fused in-frame with the histone H2B homolog *his-11* to produce pJH4.52 (G. Seydoux, personal communication). This gene was placed under control of the *pha-4* promoter, nucleotides 31–10,967 of cosmid F38A6 (M. Horner and S.E.M., unpublished; Horner *et al.*, 1998). **GFP-PM** carries GFP from pPD 95.85 (http://www.ciwemb.edu; Fire *et al.*, 1990) with the isoprenylation sequence of *mig-2* (Zipkin *et al.*, 1997) added to the carboxyl terminus: TCAAGCCACAAAAGAAGAAGAAGTCTTGCAACATCATGTAG (which encodes KPQKKKKSCNIMstop). GFP-PM is also under control of the *pha-4* promoter (M. Horner and S. E. M., unpublished; Horner *et al.*, 1998). Both of these constructs were microinjected into *C. elegans* (Mello and Fire, 1995) by using the following injection mix: 20 ng/μl GFP construct, 100 ng/μl sheared herring sperm genomic DNA, 30 ng/μl 1-kb ladder (Gibco BRL), and 100 ng/μl pRF4, which permits identification of transgenic animals because they roll (Mello *et al.*, 1991). Both constructs were stably integrated into the genome by using standard protocols (Mello and Fire, 1995) to generate *pxIs6* and *pxIs7* for GFP-N and GFP-PM, respectively.

Microscopy and Laser Ablations

Embryos were collected from gravid adult hermaphrodites into M9 (Brenner, 1974) and transferred to 4% agar pads on standard microscope slides. For time-lapse microscopy, we used a Zeiss Axioskop microscope equipped with Nomarski DIC optics. For laser ablation, blastomeres were irradiated with the 440-nm laser beam as described previously (Avery and Horvitz, 1987; Horner *et al.*, 1998). Blastomeres were treated with laser light for 15–30 s at 2–5 pulses per second until the nuclei could be seen bubbling.

Time-Lapse Microscopy

Time-lapse microscopy was used for lineage analysis of pharyngeal and buccal cavity cells and for following cell movements and shape changes during pharyngeal morphogenesis. A cooled Princeton Instruments digital camera was used to capture images with OpenLab software (Improvision). Ten optical sections were taken per time point; each section was approximately 2 microns offset from the previous section. Time points for differential interference microscopy were taken every 30 s and for GFP, every 10–15 min at 1% power (100 W Attoarc).

Immunostaining

Immunostaining was performed similar to previous reports (Albertson, 1984; Mango *et al.*, 1994). Gravid hermaphrodites were allowed to lay embryos overnight on 10-cm plates. The mothers and hatched larvae were then removed by rinsing the plates with M9. Embryos were harvested by gently scrubbing the plates and suctioned by using a 1-ml pipette. Embryos were transferred to a watch glass and allowed to settle. Debris was removed from the watch glass with a 1-ml pipette without disturbing the embryos. Embryos were then placed on poly L-lysine coated slides. Coverslips were placed on top of the embryos and excess M9 was wicked away until the eggshells were cracked open. The slides were placed on dry ice for 10 min, the coverslips removed rapidly, and the slides immersed in methanol on dry ice for 5 min. The slides were transferred to a coplin jar containing acetone on dry ice for an additional 5 min, and then passed through a rehydration series for 30 s each in 90, 60, 30, and 10% acetone in water. The slides were rinsed and stored in TNB solution (Mango *et al.*, 1994) for 30 min. Mouse anti-JAM-1 antibodies (MH27; Francis and Waterston, 1991) and rabbit anti-GFP antibodies (Clontech) diluted in TNB were then incubated with the embryos for 2–4 h at room temperature. The slides were washed in TBS (20 mM Tris-HCl, pH 8.0, 150 mM

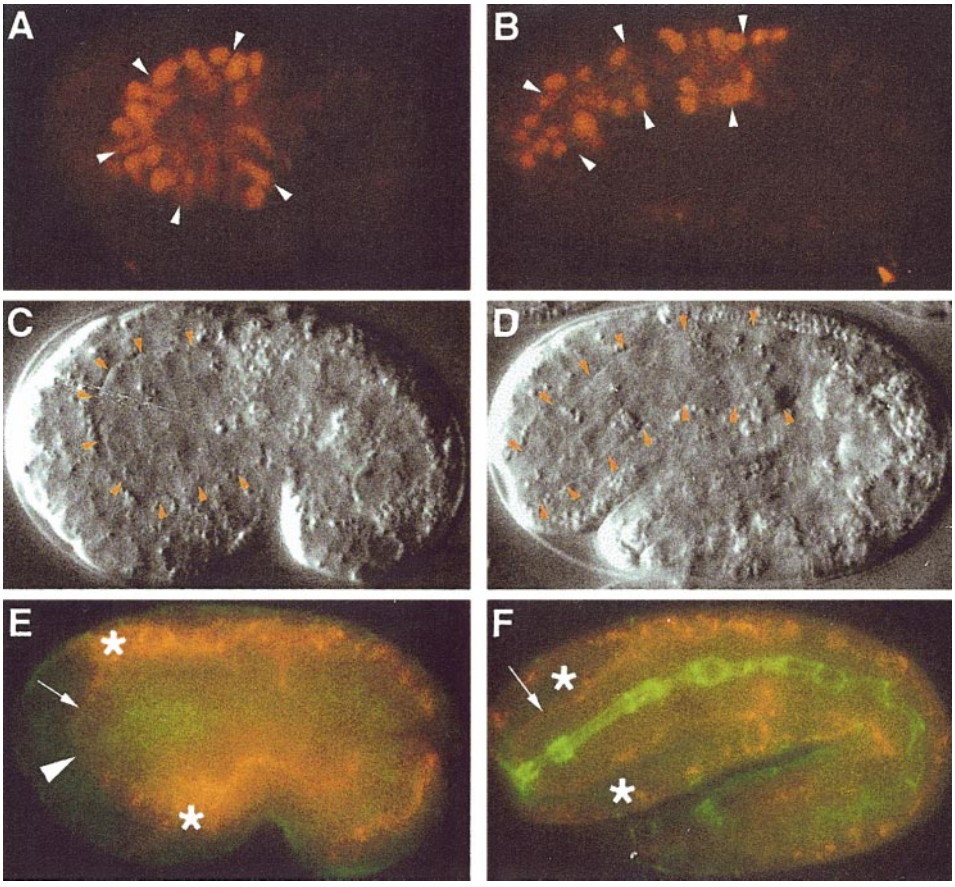

FIG. 1. Pharyngeal extension. Embryos before (A, C, E) and after (B, D, F) pharyngeal extension. (A, B) Embryos immunostained with αPHA-4 antibodies, to highlight the pharynx (arrowheads; Horner *et al.*, 1998). (C, D) Images of similarly staged embryos by differential interference contrast (DIC) microscopy. Red arrowheads mark the basement membrane surrounding the pharynx primordium. (E, F) Embryos immunostained with antibodies directed against the basement membrane collagen LET-2 (red; AT-68; Sibley *et al.*, 1994; Graham *et al.*, 1997) and an adherens junction protein JAM-1 (green; MH27; Francis and Waterston, 1991). LET-2 is synthesized in body wall muscle cells (*) and deposited on neighboring basement membranes (arrow points to the LET-2 stain, arrow head points to a gap in staining at the anterior edge of the primordium, see text for details; Graham *et al.*, 1997). Note that the pharynx, midgut, and rectum all express the adherens junction marker. Each embryo is ~50 μm long.

NaCl) (Albertson, 1984) for 15 min before incubation with FITC or Cy3-conjugated secondary antibodies (Jackson Immunologicals). Slides were incubated for an additional 2–4 h at room temperature, washed in TBS for 15 min, and mounted with 15 μl of mounting medium (1 mg/ml *p*-phenylenediamine, 50% glycerol, 1.5 mg/ml sodium citrate, and 6.0 mg/ml sodium phosphate). The edges of the coverslips were sealed with nail polish and analyzed under the microscope.

RESULTS

Pharyngeal morphogenesis initiates approximately 330 min after the first embryonic cell division, when 78 of the 80 pharyngeal cells have been born and the embryo has begun to elongate. At this time, the pharyngeal precursors form a compact primordium deep within the embryo. Pharyngeal extension occurs over the next 60 min, when the pharyngeal precursors alter their morphology and position to form a linear tube linked to the buccal cavity at the anterior (Figs. 1B, 1D, and 1F).

We used three reporter constructs to follow the behavior of the pharyngeal precursors during extension (Fig. 2; see Materials and Methods). The first, GFP-PM, targets GFP to the plasma membrane using the isoprenylation sequence of *mig-2* (Zipkin *et al.*, 1997). This construct enabled us to observe the shape of cells during extension. The second, GFP-N, localizes GFP to the nucleus with a fusion to *his-11*, a histone 2B homologue (Seydoux, personal communication; J. Waddle, personal communication). This construct facilitated lineage analysis and cell identification (see Materials and Methods). Both of these genes are under control of the *pha-4* promoter, which is selectively ex-

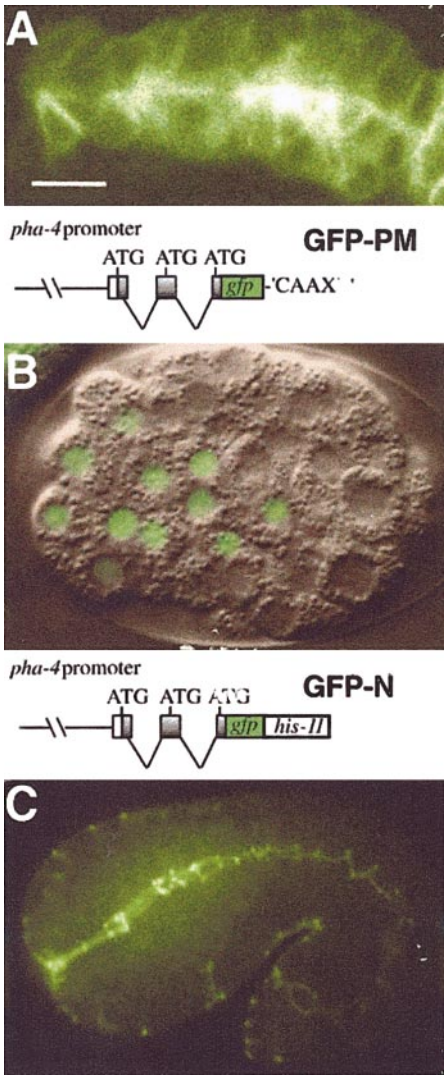

FIG. 2. GFP markers. Green fluorescent protein constructs used in this study: GFP-PM, which is targeted to the plasma membrane of cells in the digestive tract, is shown here in the pharynx of a twofold stage embryo (A). Overlay of DIC and fluorescence images of an early embryo (~100 cell stage) expressing the nuclear GFP-N construct (B) and fluorescence micrograph showing JAM-1::GFP localized to adherens junctions within the digestive tract (C; Mohler *et al.*, 1998). Bar = 5 μm; a full-sized embryo is ~50 μm long.

pressed in the digestive tract, including all pharyngeal and buccal cavity cells (Horner *et al.*, 1998). The third construct, JAM-1::GFP (Mohler *et al.*, 1998), targets GFP to adherens junctions (Francis and Waterston, 1991; Hall, Pers. Comm.) and was used to locate the apical surface of cells. These constructs provided a means to follow the different steps of pharyngeal extension in living, unfixed embryos.

Here, we focus on the behavior of the cells that ultimately form the anterior pharynx and the buccal cavity since these cells appear to play a critical role during pharyngeal extension (described below). Although these cells do not differentiate until hours after extension, we refer to them according to the cell type they eventually become (e.g., epithelial cell "e1D," which derives from the ABaraaaapap blastomere; Sulston *et al.*, 1983).

The Pharyngeal Primordium

Prior to pharyngeal extension, the pharyngeal cells appear wedge-shaped with their apical surfaces, as defined by JAM-1::GFP expression, located at the tip of the wedge and their basolateral compartment extending over the remaining surfaces (Figs. 3A, 3C, and 3E). The cells' apicobasal polarity is aligned along the rostrocaudal axis of the embryo with the apical surface facing posterior and the basal surface flanking the basement membrane at the anterior. Cell-lineage analysis with GFP-N demonstrated that these wedge-shaped cells include the e1 and e2 subclasses of pharyngeal epithelial cells (for stages and cell names, see Sulston *et al.*, 1983). Cells located posterior to the pharyngeal epithelial cells are organized with their apicobasal polarity oriented along the dorsoventral axis of the embryo and their apical surfaces facing the midline of the pharyngeal primordium (Figs. 3C and 3D); the midline will ultimately become the pharyngeal lumen. This arrangement implies that the pharyngeal epithelial cells effectively "cap" the nascent pharyngeal lumen, thereby blocking the pharyngeal tube from extending to the exterior.

The pharyngeal primordium is surrounded by a basement membrane that separates the pharyngeal cells from the rest of the embryo. The basement membrane can be detected by light microscopy as a gap between the pharyngeal cells and other cells of the head (Fig. 1C). By antibody staining, the anterior section of basement membrane differs from the remainder since it fails to stain for α-collagen IV (Fig. 1E). This may reflect an absence of a basement membrane at the anterior (or of collagen) or, alternatively, a different organization that masks the antigenic epitopes.

The pharyngeal epithelial cells are located approximately three cell diameters from the anterior of the embryo (~11.1 $\pm$ 0.5 μm, n = 5). This area is filled with cells that ultimately contribute to the buccal cavity and epidermis (Figs. 3A and 3B; Figs. 4A and 4B). Anterior to the pharyngeal epithelial cells lie nine arcade cells that become organized into two rings called the anterior and posterior arcades. These cells make up the anterior two-thirds of the buccal cavity; the remainder of the buccal cavity is comprised of pharyngeal epithelial cells (Albertson and Thomson, 1976; Wright and Thomson, 1981). To simplify the nomenclature, we use the term "buccal cavity" to refer to the structure made by the arcade cells alone. Anterior to the arcade cells lie epidermal cells that link the digestive tract to the epidermis surrounding the embryo.

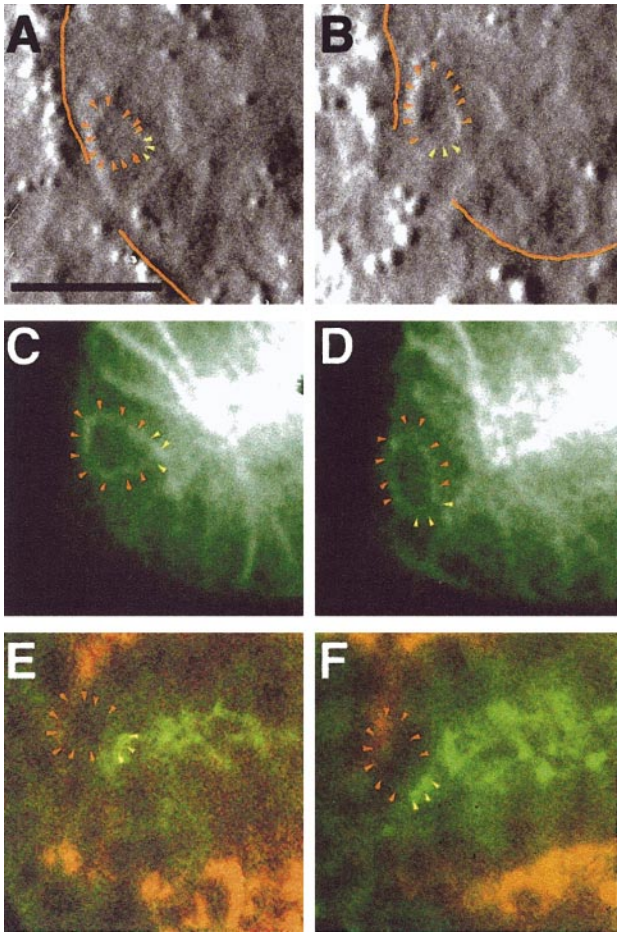

FIG. 3. Stage I reorientation of the pharyngeal epithelial cells. (A, B) DIC images of the pharyngeal epithelial cells before (A) and after (B) reorientation. The basement membrane that surrounds the pharynx primordium is outlined in red. (C, D) The equivalent region of an embryo expressing GFP-PM to highlight the cells' plasma membranes. (E, F) Embryos stained for the basement collagen protein LET-2 (red; Sibley *et al.*, 1994; Graham *et al.*, 1997) and adherens junction marker JAM-1 (green; Francis and Waterston, 1991). At the beginning of pharyngeal extension (A, C, E), the pharyngeal epithelial cells are wedge-shaped with their tiny apical surfaces facing the posterior of the embryo (yellow arrowheads) and their basolateral surfaces covering the bulk of the cell surface (red arrowheads). Over the next 15 min (B, D, F), the cellular junctions appear to rotate so that the apical surfaces are located more anteriorly and the nascent pharyngeal lumen abuts the basement membrane. Bar = 5 μm.

Three Stages of Pharyngeal Extension

Pharyngeal extension can be loosely divided into three stages: (1) reorganization of cellular polarity within the pharyngeal epithelial cells, ("Reorientation"), (2) formation of an epithelium by the arcade cells ("Epithelialization"), and (3) movement of the pharynx anteriorly and the epidermis of the mouth posteriorly ("Contraction"). These cellular behaviors produce an epithelial tube that links the digestive tract to the exterior of the animal.

Pharyngeal extension begins when pharyngeal epithelial cells located in the anterior of the pharyngeal primordium adjust the apicobasal polarity of their membranes to lie parallel to the dorsoventral axis of the embryo (Fig. 3). Prior to the first stage, the apicobasal axes of these cells are generally aligned with the rostrocaudal axis of the embryo (Figs. 3A, 3C, and 3E). During reorientation, the epithelial cells shift their apical surfaces 30–90° to align their apicobasal axes with the dorsoventral axis (Figs. 3B, 3D, and 3F). We observed this reorientation using several markers of apical polarity including JAM-1::GFP, endogenous JAM-1, and the atypical protein kinase C homologue PKC-3 (Wu *et al.*, 1998). Thus, polarity of the entire cell is affected during reorientation rather than relocalization of a single marker. One interesting possibility is that the whole cell rotates toward the anterior of the embryo (i.e., clockwise for dorsal cells and counterclockwise for ventral cells). Alternatively, cells may reorganize polarity by repositioning their apical junctions within a stationary membrane. We have not distinguished between these possibilities and do not favor one over the other.

We quantified reorientation by comparing the distances traveled by the apical and basal surfaces of the pharyngeal epithelial cell e1D. Whereas the apical surface of e1D moved ~2.5 μm closer to the future mouth of the embryo, the basal surface did not change position (Table 1). These

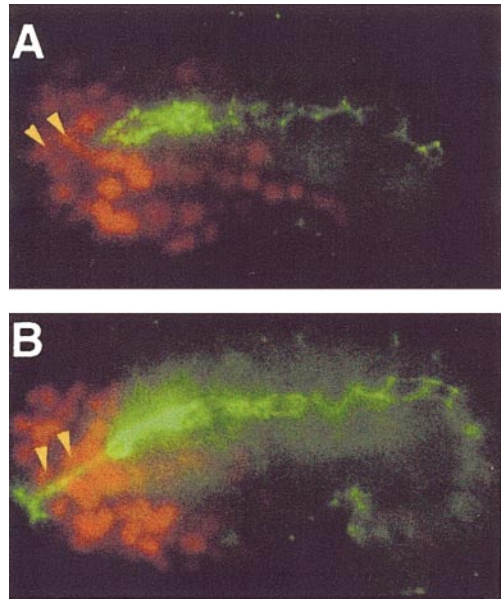

FIG. 4. Stage II epithelialization of the arcade cells. The arcade cells (arrows) before (A) and after (B) formation of adherens junctions. Embryos stained for adherens junctions in green (MH27; Francis and Waterston, 1991) and nuclei in red (DAPI).

TABLE 1

Movement of Pharyngeal Epithelial Cell e1D during Pharyngeal Extension

Distance from embryo anterior to:	Prerotation (t = 0)	Stage I (t = 10 min)	Stage III (t = 50 min)
e1D Apical Surface[a]	12.7 ± 0.7 μm	10.3 ± 0.1 μm	6.4 ± 0.5 μm
e1D Basal Surface[b]	10.9 ± 0.5 μm	10.9 ± 0.3 μm	8.6 ± 0.4 μm

[a] The distance from the apical surface of the cell (as determined by JAM-1::GFP) to the anterior edge of the embryo.

[b] The distance from the center of the basal surface of the cell (as determined by DIC optics) to the anterior edge of the embryo. Note that after the 50-min time point, the pharyngeal cells continued to extend anteriorly; however, embryonic movements interfered with making accurate measurements.

events occur rapidly, within a 10-min time frame beginning approximately 330 min after the first embryonic cleavage. Similar movements were observed for neighboring pharyngeal epithelial cells (Fig. 3). The net result of reorientation is that the apical surface of the pharyngeal primordium, and essentially the future lumen of the pharynx, is positioned more anteriorly and abuts the arcade cells. Importantly, these data demonstrate that this change depends on reorganization of cell polarity and not displacement of cells toward the anterior.

During the second phase of pharyngeal extension, a continuous epithelium is formed between the pharyngeal cells, the arcade cells, and the anterior epidermis (Fig. 4). Prior to this stage, only the pharynx and epidermis contain adherens junctions, as assayed by staining for JAM-1 or JAM-1::GFP. During a 10-min interval, faint puncta of JAM-1::GFP appear within the arcade cells (data not shown). The puncta are rapidly converted into a continuous belt of JAM-1::GFP, which likely reflects polarization of the arcade cells and adhesion between these cells and the neighboring pharyngeal and epidermal cells (Fig. 4). The atypical protein kinase C homologue PKC-3 (Wu *et al.*, 1998) is localized to the apical surface with similar timing as JAM-1::GFP (data not shown). We suggest that formation of a continuous epithelium provides mechanical coupling between the pharynx, the buccal cavity, and the epidermis.

During the third stage of pharyngeal extension, the pharynx shifts anteriorly and the epidermis moves posteriorly (Figs. 5A–5D). For example, e1D shifts 2–4 μm towards the anterior during the first 30 min of Stage III: its apical surface moves 3.9 μm (n = 8) while its basal surface moves approximately 2.1 μm (n = 8) (Table 1). These data illustrate that the entire cell moves anteriorly, and also that the cell elongates along its anteroposterior axis. Pharyngeal cells neighboring e1D behave similarly, which generates a row of elongated cell bodies within the anterior pharynx. At the same time that the pharyngeal cells move forward, the epidermal cells shift posteriorly. This behavior is most easily observed as an indentation at the tip of the embryo that eventually stretches 4.5 μm inward (Figs. 5A–5D). The intervening arcade cells become progressively more wedge-shaped during contraction, as their apical surfaces shrink dramatically (Figs. 5G–5J). Ultimately, the anterior tips of the pharyngeal epithelial cells intercalate between the arcade cells, thereby bringing the pharyngeal primordium further forward. These movements are largely complete within 1 h.

A Model for Pharyngeal Extension

We considered two mechanisms to explain the forces that drive pharyngeal extension. First, the anterior pharyngeal cells might "pull" the pharynx primordium anteriorly. This model, which is based on the cellular movements described above, proposes that, once a continuous epithelium is generated between cells of the anterior pharynx, buccal cavity, and epidermis, a local contraction brings the apical surfaces of these cells close together and pulls the rest of the pharynx forward. An alternate explanation is that cells located in the posterior of the pharynx primordium "push" the anterior pharynx forward to reach the buccal cavity. This model is based on changes in the shape of the posterior pharynx primordium during extension. The posterior pharynx elongates 2.3 ± 0.3 μm (n = 5) along its anteroposterior axis and shrinks 1.7 ± 0.6 μm (n = 6) along its dorsoventral axis (Table 2; Figs. 1 and 4; data not shown).

To distinguish between the pulling and pushing models, we blocked posterior pharynx development and followed the behavior of the anterior pharyngeal cells. Since most of the posterior pharynx derives from the MS blastomere at the eight-cell stage (Sulston *et al.*, 1983), we used genetic or physical approaches to destroy the MS blastomere or its granddaughters, MSaa and MSpa.

Two lines of evidence demonstrate that MS-derived pharyngeal cells are not required for pharyngeal extension. First, we used laser ablation to destroy MSaa and MSpa. In successfully ablated embryos, no posterior pharynx was seen by light microscopy or with GFP-PM, and only one subsequent round of cell division occurred in the treated cells. Despite the loss of the MS-derived pharyngeal cells, pharyngeal extension occurred normally (Fig. 6B). We observed reorientation of polarity, epithelialization, and contraction, similar to unablated embryos (n = 4). These embryos arrested at the twofold stage with pharynges that resembled the anterior of a normal twofold embryo. As a second approach, we analyzed pharyngeal extension in *pop-1(zu189)* embryos. The HMG protein POP-1 is required to specify anterior fates, including that of the MS blastomere (Lin *et al.*, 1995, 1998). In mutant *pop-1* embryos, the MS blastomere develops like its posterior sister, the E blastomere, and produces excess midgut cells instead of pharyngeal cells (Lin *et al.*, 1995). Nevertheless, the pharyngeal primordium underwent normal extension in these mutants, ultimately producing the elongated shape of a normal pharyngeal tube (Fig. 6E). These data demonstrate that MS-derived pharyngeal cells are not required for pha-

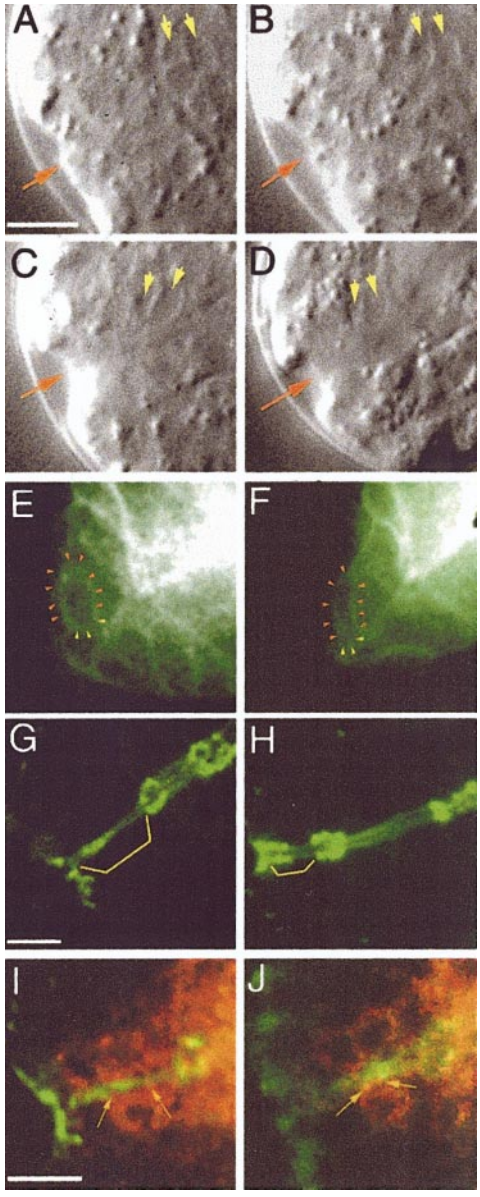

FIG. 5. Stage III contraction of the buccal cavity and the pharyngeal epithelial cells. (A–D) DIC images showing the pharyngeal epithelial cells (yellow arrows) and epidermal cells (red arrow) during Stage III contraction. Note that the epidermal cells move posteriorly while the pharyngeal epithelial cells shift anteriorly and become elongated. (E, F) Pharyngeal epithelial cell e1D in a GFP-PM-expressing embryo before (E) and after (F) Stage III contraction. The apical surface is marked with yellow arrowheads and the basolateral surfaces are red. (G–I) Before (G, I) and after (H, J) Stage III contraction. The length of the apical surfaces of the arcade cells is reduced during contraction (brackets in G and H), as measured by MH27 staining (green; Francis *et al.*, 1991). Individual arcade cells are highlighted by arrows in I and J. Concomitant with these events, the sister of e1D, ABaraaaapaa, dies and its corpse slips between the arcade cells and disappears (Sulston *et al.*, 1983; M. P. and S. E. M., unpublished observations). The pharyngeal epithelial cells appear to follow the corpse between the arcade cells (data not shown). Bar = 5 μm.

TABLE 2

Dimensions of the Posterior Pharynx during Pharyngeal Extension

	Prerotation (t = 0)	Stage III (t = 50 min)
Length of A/P axis	11.5 ± 1.6 μm	13.7 ± 1.8 μm
Length of D/V axis	17.3 ± 1.0 μm	15.6 ± 0.9 μm

Note. The length of the posterior pharynx was measured along the anteroposterior axis from the tip of the pm3 pharyngeal muscle precursors to the posterior tip of the pm8 pharyngeal muscle precursor. The width of the posterior pharynx was measured along the dorsoventral axis of the embryo at the position of the pm4 and pm5 pharyngeal muscle precursors. For the names of individual pharyngeal cells, see Albertson and Thomson (1976).

ryngeal extension and favor the pulling hypothesis of pharyngeal extension.

The pulling hypothesis predicts that tension between the pharynx, buccal cavity, and epidermis is used to pull the entire pharynx forward. To test this idea, we destroyed the arcade cells by laser ablation and examined the behavior of the neighboring pharyngeal cells (Fig. 7). As expected, the arcade cells failed to epithelialize after treatment, indicating that the ablation was successful. We observed reorientation of the pharyngeal epithelial cells, but no movement of the pharynx primordium toward the mouth (n = 3). Moreover, we observed a decrease in the posterior movement of the epidermis and consequently a smaller indentation in treated embryos. These data are consistent with the idea that epithelial connections between the pharynx, buccal cavity, and epidermis are required to generate the force that pulls the pharynx forward and the buccal cavity backward.

DISCUSSION

We have described the cellular behaviors that accompany the early stages of pharyngeal morphogenesis. Our studies demonstrate that conversion of the pharynx from a ball to a tube depends on generating an epithelium that links anterior pharyngeal cells to the buccal cavity and surrounding epidermis. Formation of an epithelium during Stages I and II probably provides the mechanical strength to pull the pharynx forward during Stage III. We hypothesize that the force to pull the pharynx forward is produced by a local contraction between the pharyngeal epithelial cells, the buccal cavity, and the epidermis (see model, Fig. 8). These behaviors are strikingly different from those involved in other morphogenetic processes such as cell migration or convergent extension during vertebrate gastrulation and neurulation. Rather, the behaviors we observe resemble aspects of kidney tubulogenesis, suggesting that an understanding of pharyngeal extension may help us understand morphogenesis of other, more complex, organs.

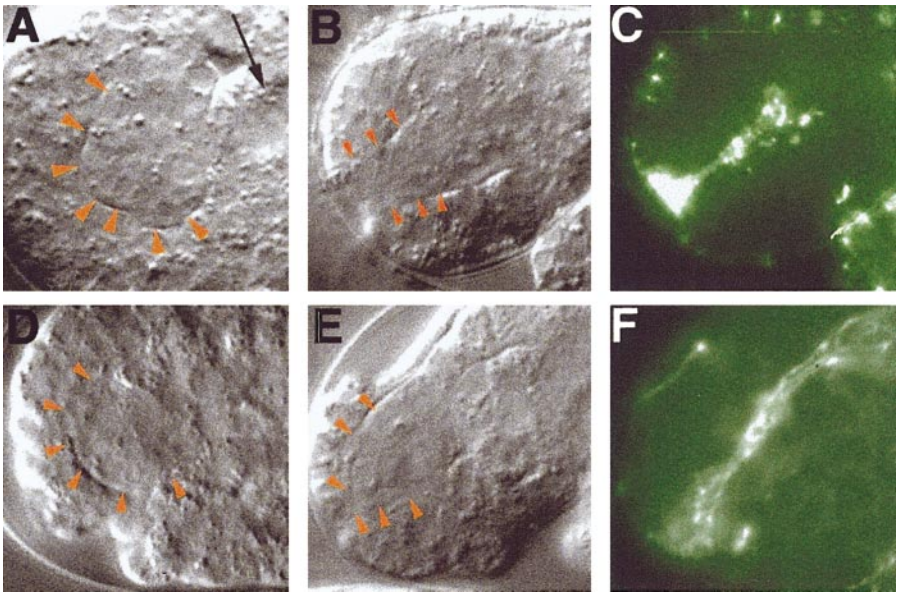

FIG. 6. MS-derived pharyngeal cells are not required for pharyngeal extension. (A–C) The pharynx primordium before (A) and after (B, C) pharyngeal extension in an embryo in which the MSaa and MSpa blastomeres were destroyed by laser ablation. The outline of the pharynx is highlighted by red arrowheads. A band of the adherens junction marker MH27 suggests that the epidermis, buccal cavity, and pharynx form a continuous epithelium despite the absence of the posterior pharynx (C). The same embryo is shown in A and B. A black arrow denotes the ablated blastomeres in A. (D–F) A *pop-1* embryo before (D) and after (E, F) pharyngeal extension. Pharyngeal extension appears to occur despite the absence of the posterior pharynx. (F) MH27 staining (Francis and Waterston, 1991) indicates the presence of a continuous epithelium.

Pharyngeal Extension in C. elegans

Stage I: Reorientation. During the first stage of pharyngeal extension, pharyngeal epithelial cells reorient their apicobasal polarity from rostrocaudal to dorsoventral relative to the embryonic axes. This rearrangement alters the morphology of the pharynx from a cyst, with the apical surfaces located internally, to a short tube that extends from the midgut to the anterior edge of the pharyngeal primordium. Importantly, this movement aligns the pharyngeal epithelial cells with the arcade cells, enabling a continuous epithelium to form during Stage II. At present, two models can explain how reorientation might occur. First, reorientation might reflect rotation of the entire cell. For example, the basement membrane could provide a substratum that would promote cell turning in a clockwise or counterclockwise direction. In the second model, junctions within a stationary cell might be relocated to the anterior. That is, disassembly/reassembly or sliding of junctional components could physically move the apical compartment forward. Evidence for both kinds of events exist in other organisms. For example, dissociated sea urchin cells form cysts *in vitro* with their apical membranes located internally. They achieve this configuration by rotating individual cells within an aggregate of randomly oriented cells (Nelson and McClay, 1988). On the other hand, Madin–Darby canine kidney (MDCK) cells depolarize their membranes during tubulogenesis *in vitro* and gradually

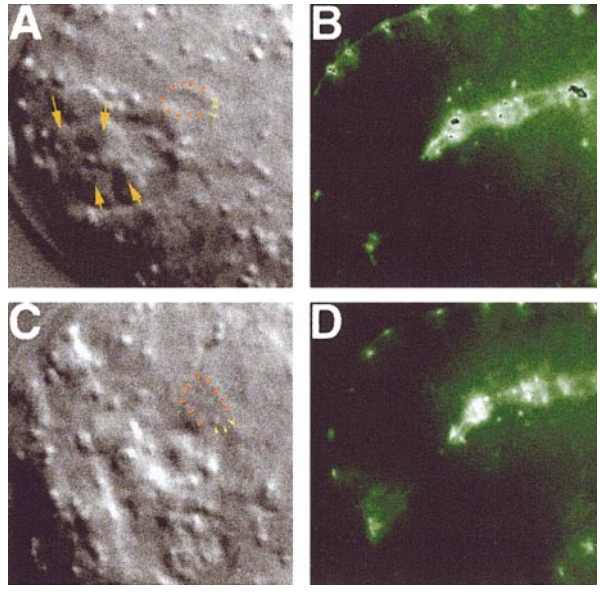

FIG. 7. Pharyngeal extension depends on the arcade cells. Pharyngeal epithelial cells before (A, B) and after (C, D) pharyngeal extension. The arcade cells were destroyed by laser ablation, as monitored by the appearance of debris (orange arrows in A) and the absence of adherens junctions (B, D). The apical surface of the pharyngeal epithelial cell e1D rotated anteriorly (yellow arrowheads in A and C), but no cell elongation or forward movement were observed. Red arrowheads depict the basolateral surface of e1D in A and C.

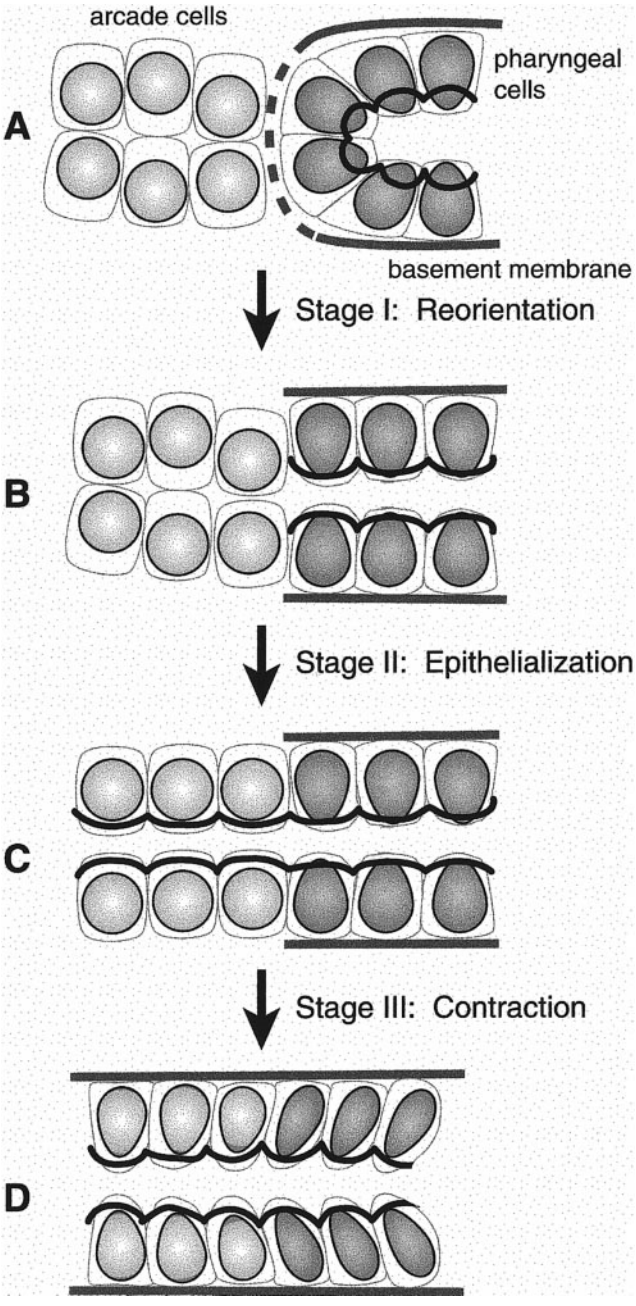

FIG. 8. Summary of pharyngeal extension. Prior to pharyngeal extension, the pharyngeal primordium forms an epithelialized cyst deep within the embryo (A). The pharyngeal primordium and arcade cells appear to be separated by a basement membrane at this time (dotted line). During Stage I "Reorientation" (A to B), anterior pharyngeal cells reorient their apicobasal polarity to "uncap" the cyst and form a tube. During stage II "Epithelialization" (B to C), the arcade cells epithelialize and produce a continuous epithelium that is linked to the epidermis anteriorly (not shown) and the pharynx posteriorly. Finally, during stage III "Contraction" (D), the apical surfaces of the arcade and anterior pharyngeal cells constrict as these cells are brought in close apposition to each other. This constriction apparently pulls the pharynx toward the anterior of the animal.

rebuild their junctions within stationary cells to generate tubes with appropriate polarity (Pollack *et al.*, 1998). Similarly, adherens junctions in *C. elegans* epidermal cells are regulated dynamically during cell migration and fusion (Podbilewicz and White, 1994; Williams-Masson *et al.*, 1998; Chin-Sang and Chisholm, 2000).

In addition to the polarity changes observed during Stage I, cells located at the anterior tip of the pharyngeal primordium presumably lose cell contacts with some of their neighbors. This alteration is required to remove the physical barrier that these cells impose between the nascent pharyngeal lumen and the developing buccal cavity. The mechanisms that underlie this behavior are currently unknown, but could involve differential adhesiveness between cells. For example, both pharyngeal cells and arcade cells express members of the cadherin family of adhesion molecules, suggesting these proteins could play a role in adhesion-mediated rotation (Pettitt *et al.*, 1996; Costa *et al.*, 1998; M.P. and S.E.M., unpublished observations). In *C. elegans* epidermal cells, a cadherin/catenin system maintains the association of actin filaments with adherens junctions, which is important for proper body morphogenesis (Costa *et al.*, 1998; Raich *et al.*, 1999). Surprisingly, however, embryos mutant for components of the cadherin/catenin system appear virtually unaffected in cell adhesion, apicobasal polarity, adherens junction formation, or pharyngeal extension (Pettitt *et al.*, 1996; Costa *et al.*, 1998; M. P. and S. E. M., unpublished observations). One possibility is that overlapping expression of different cadherin/catenin family members compensates for the loss of a single protein. The cadherin family is large in *C. elegans*, with 4 catenin homologues and 15 genes containing cadherin-type repeats.

Stage II: Epithelialization. During the second stage of pharyngeal extension, the buccal cavity forms adherens junctions that connect the buccal cavity to the pharynx and epidermis. As a consequence, the epidermis and digestive tract form a continuous epithelium that topologically resembles a cored apple, with the epidermis defining the surface of the apple and the digestive tract making up the core. This structure is under tension, such that disruption of the epithelium in one area releases tension throughout the embryo, including regions of the embryo that are distant from the initial lesion (M.P. and S.E.M., unpublished observations). This behavior may explain why mutants that disrupt embryonic elongation also affect pharyngeal morphogenesis (S.E.M., unpublished observations).

What factors are required to build the digestive tract epithelium? Surprisingly, many proteins implicated in the formation or maintenance of epithelia in other animals are apparently not required in the *C. elegans* digestive tract. For example, homologues of Crumbs, cadherins, discs-large, zo-1, α or β integrins do not give rise to obvious pharyngeal defects after being inactivated (Williams and Waterston, 1994; Pettitt *et al.*, 1996; Baum and Garriga, 1997; Costa *et al.*, 1998; M.P. and S.E.M., unpublished observations; G. Herman and J. R. Priess, personal communication.; see

Drubin and Nelson, 1996 and Yeaman *et al.*, 1999 for reviews on epithelial polarity). There are three potential caveats associated with these inactivation experiments: genetic redundancy, maternal rescue, and incomplete loss-of-function. Nevertheless, the list of genes is surprisingly long and suggests that novel protein families may play a role in pharyngeal extension.

A few loci that regulate epithelial cell fate or function have been tentatively identified by screening chromosomal deficiencies for those that affect the embryonic epidermis (Chanal and Labouesse, 1997; Labouesse, 1997; Terns *et al.*, 1997). This approach led to the recent discovery of *let-413*, which is deleted by *sDf35* and is critical for proper adherens junction formation or positioning. LET-413, which contains a PDZ motif and leucine-rich repeats similar to *Drosophila* scribble, is localized to basolateral membranes of all epithelial cell types, including the pharynx, where it plays a role in organizing cell polarity (Legouis *et al.*, 2000). Other molecules required to specify pharyngeal epithelial cells or build their epithelial junctions have not yet been found.

Stage III: Contraction. During the third stage of pharyngeal extension, cells of the pharynx, buccal cavity, and epidermis appear to undergo a local contraction that pulls them tightly together. The remainder of the pharynx is presumably dragged forward by virtue of its attachment to the anterior pharynx. This hypothesis is based on the observation that the pharynx, buccal cavity, and epidermis form a continuous epithelium that appears to be under tension during pharyngeal extension. During Stage III, movement of the pharynx forward is matched by movement of the epidermis backward. These behaviors depend on the arcade cells since ablation of the arcade cells disrupts movement in either direction. Interestingly, when we ablate the midgut or posterior pharynx, the pharynx shifts even more anteriorly, the pharyngeal epithelial cell bodies fail to elongate extensively, and posterior movement of the epidermis is aborted (Fig. 6). These behaviors can be explained if, normally, cells of the pharynx, buccal cavity, and mouth undergo a contraction that is resisted by tension from the entire digestive–epidermal epithelium.

The Stage III contraction may occur by a "purse-string" mechanism, similar to what has been proposed for other morphogenetic events. The purse-string model has been implicated in sealing epithelial sheets during wound healing, dorsal closure in *Drosophila*, and ventral closure in *C. elegans* (Knust, 1997; Nodder and Martin, 1997; Williams-Masson *et al.*, 1997). This model proposes that cells at the leading edge of a gap in an epithelium are linked to one another by a circumferential ring of actin and myosin. The actin/myosin cable is tethered to adherens junctions by cadherin/catenin complexes, which maintain the actin/myosin cables in register from cell to cell (Gumbiner, 1996). As the cable contracts, the cells are pulled together until the gap is sealed. By analogy, the epithelial connections between the *C. elegans* pharynx, buccal cavity, and epidermis may enable these cells to form an apically localized actin/myosin bundle that pulls these cells close together. Consistent with this idea, stains with fluorescently labeled phalloidin have shown that the apical surfaces of the pharynx, buccal cavity, and epidermis are highly enriched with actin (M. P. and S.E.M., unpublished observations). We note, however, that the behavior of the cells during pharyngeal extension differs from a traditional purse-string in that the contraction appears to be localized to a small region of the entire epithelium and does not encompass a hole in the epithelium. In addition, movement proceeds more slowly than do other characterized purse-string closures. Whereas ventral closure in *C. elegans* occurs at a rate of ~1.0 μm/min (Williams-Masson *et al.*, 1997), pharyngeal cells move at a rate of ~0.3 μm/min (M. P. and S.E.M., unpublished observations).

Is Signaling Involved in Pharyngeal Extension?

In other organisms, changes in cell polarity can be induced by extrinsic sources such as cell–substratum attachment and cell–cell adhesion or signaling (Hogan, 1999; Yeaman *et al.*, 1999). The behavior of the arcade and pharyngeal epithelial cells raises the interesting possibility that signaling might coordinate the morphogenetic events of pharyngeal extension. For example, the arcade cells might induce reorientation of pharyngeal epithelial cells or pharyngeal epithelial cells might induce epithelialization of arcade cells. The timing of these events is consistent with communication between these groups of cells. For example, epithelialization of the arcade cells initiates immediately after reorientation of the pharyngeal epithelial cells. Our laser ablation studies do not support this hypothesis, however, since we have not seen the predicted phenotypes after treatment (Fig. 7, and data not shown). For example, laser ablation of the pharyngeal epithelial cell precursor ABaraaaa at the 4E stage of embryogenesis does not block epithelialization of the arcade cells (M.P. and S.E.M., unpublished observations). These experiments are not definitive, however, as it is difficult to be certain that all arcade cells or all pharyngeal epithelial cells have been destroyed, given their small size and internal location in the embryo. If a single cell remained after laser ablation, it might be sufficient to send a signal.

Many molecules have been identified that play a role in signaling during organogenesis and tubulogenesis. For example, ligands of the *wnt* (Kuure *et al.*, 2000) and IL-6 (Barasch *et al.*, 1999) family probably mediate ureteric bud signaling to the mesenchyme. Interestingly, *wnt* signaling has also been implicated in early and late stages of pharyngeal development (Bowerman, 1998; A. Paulson and S.E.M., unpublished observations). FGF has also been implicated in organ morphogenesis including *Drosophila* trachea and the mammalian lung (Metzger and Krasnow, 1999). In *C. elegans*, a member of the FGF family, *egl-17*(Burdine *et al.*, 1997), is expressed in anterior epidermal cells at the onset of pharyngeal extension (M.P. and S.E.M., unpublished observations). However, we have not observed defects in pharyngeal extension after inactivation of *egl-17* alone or in

combination with *let-756* (Roubin *et al.*, 1999); the only other known FGF homologue in *C. elegans* (M.P. and S.E.M., unpublished observations). Further genetic studies are needed to address the potential role of signaling during pharyngeal extension.

Pharyngeal Extension Resembles Kidney Morphogenesis

The cellular behaviors described here resemble aspects of tubulogenesis in other organisms, notably the metanephric kidney. Development of the kidney depends on a series of reciprocal interactions between the ureteric bud and the surrounding mesenchyme (Saxen and Sariola, 1987; Kuure *et al.*, 2000). Organogenesis is initiated by signals in the mesenchyme that induce formation of the ureteric bud, an epithelial outgrowth from the Wolffian duct. In response, the ureteric bud branches into the ureter tree and induces the mesenchyme to condense, epithelialize, and develop nephrons. Ultimately, the ureteric and mesenchymal epithelia fuse to form the collecting tubules of the kidney.

Pharyngeal extension in *C. elegans* resembles kidney organogenesis in three ways. First, cells epithelialize in both organs to form tubes *de novo*. In worms, the arcade cells generate an epithelium that eventually gives rise to the buccal cavity, whereas metanephric mesenchyme in the kidney epithelializes to form nephrons. This process contrasts with other mechanisms for generating tubes such as budding or invagination, both of which build new structures from preexisting epithelia. For example, during branching morphogenesis in *Drosophila* trachea and mammalian lungs, cells bud from an epithelial sheet or tube, and migrate to new locations that establish the branches of the pulmonary tree (Metzger and Krasnow, 1999).

The second similarity between pharyngeal extension and kidney morphogenesis is that the tubes are composed of newly formed as well as preexisting epithelia that fuse into a continuous structure. In nematodes, the anterior digestive tract is produced from the pharyngeal primordium, which forms an epithelium before the onset of morphogenesis, and the newly formed buccal cavity epithelium. In the kidney, the ureteric bud epithelium fuses with mesenchymally produced S-shaped bodies to form the collecting tubules. These behaviors require that new and preformed epithelia align with one another, with their apicobasal polarity in register. How this occurs during pharyngeal extension is presently unknown, but could involve cell signaling, by analogy with other systems. For example, during kidney development in mammals or gonad formation in *C. elegans*, reciprocal signaling between cells allows them to coordinate the formation of extended epithelia (Newman and Sternberg, 1996; Chang *et al.*, 1999; Kuure *et al.*, 2000).

The third similarity between pharyngeal extension and kidney morphogenesis is that both organs apparently rearrange apicobasal polarity within epithelial cells as they establish new tubular structures. In *C. elegans*, the pharyngeal epithelial cells relocalize their apical surfaces to extend the nascent pharyngeal lumen towards the anterior, where they connect to the arcade cells. The cellular events associated with kidney morphogenesis, which have been studied in tissue culture models but not yet *in vivo*, suggest that apicobasal polarity is lost transiently during tubulogenesis. When MDCK cells are induced to form kidney tubules *in vitro*, apicobasal polarity is initially disrupted during budding of the nascent tube and only becomes reestablished during the final stages of tube formation (Pollack *et al.*, 1998). One important difference between the two processes, however, is that the pharyngeal epithelia apparently maintain polarity even while they change the location of their apical surfaces, whereas apical membrane polarity is lost transiently in MDCK cells (Pollack *et al.*, 1998).

In summary, we have shown that formation of the anterior digestive tract depends on forming epithelia *de novo*, which links the pharyngeal and arcade cells. A more detailed knowledge of pharyngeal extension will depend on identifying the molecules involved and understanding how they function.

ACKNOWLEDGMENTS

We thank G. Hermann, J. Priess, and J. White for unpublished information; A. Fire, J. Hardin, G. Seydoux, and J. Waddle for reagents; M. Horner for the GFP constructs; B. Bamber, M. Beckerle, J. Priess, and members of the Mango lab for comments on the manuscript. Funding to M.F.P. was provided by the National Institutes of Health Genetics Training Grant (T32-GM07464) and to S.E.M. by the National Institutes of Health (1-01-GM56264-01). S.E.M. is an assistant investigator of the Huntsman Cancer Institute Center for Children.

REFERENCES

Albertson, D. G. (1984). Formation of the first cleavage spindle in nematode embryos. *Dev. Biol.* **101,** 61–72.

Albertson, D. G., and Thomson, J. N. (1976). The pharynx of *Caenorhabditis elegans*. *Philos. Trans. R. Soc. London B Biol. Sci.* **275,** 299–325.

Avery, L., and Horvitz, H. R. (1987). A cell that dies during wild-type *C. elegans* development can function as a neuron in a *ced-3* mutant. *Cell* **51,** 1071–1078.

Avery, L., and Thomas, J. H. (1997). Feeding and defecation. In "*C. elegans* II" (D. L. Riddle, T. Blumenthal, B. J. Meyer, and J. R. Priess, Eds.), pp. 679–716. Cold Spring Harbor Laboratory Press, Cold Spring Harbor, NY.

Barasch, J., Yang, J., Ware, C. B., Taga, T., Yoshida, K., Erdjument-Bromage, H., Tempst, P., Parravicini, E., Malach, S., Aranoff, T., and Oliver, J. A. (1999). Mesenchymal to epithelial conversion in rat metanephros is induced by LIF. *Cell* **99,** 377–386.

Baum, P. D., and Garriga, G. (1997). Neuronal migrations and axon fasciculation are disrupted in *ina-1* integrin mutants. *Neuron* **19,** 51–62.

Bowerman, B. A. (1998). Maternal control of pattern formation in early *Caenorhabditis elegans* embryos. *Curr. Top. Dev. Biol.* **39,** 73–117.

Brenner, S. (1974). The genetics of *Caenorhabditis elegans*. *Genetics* **77,** 71–94.

Burdine, R. D., Chen, E. B., Kwok, S. F., and Stern, M. J. (1997). *egl-17* encodes an invertebrate fibroblast growth factor family member required specifically for sex myoblast migration in *Caenorhabditis elegans*. *Proc. Natl. Acad. Sci. USA* **94,** 2433–2437.

Chanal, P., and Labouesse, M. (1997). A screen for genetic loci required for hypodermal cell and glial-like cell development during *Caenorhabditis elegans* embryogenesis. *Genetics* **146,** 207–226.

Chang, C., Newman, A. P., and Sternberg, P. W. (1999). Reciprocal EGF signaling back to the uterus from the induced *C. elegans* vulva coordinates morphogenesis of epithelia. *Curr. Biol.* **9,** 237–246.

Chen, E. B., and Stern, M. J. (1998). Understanding cell migration guidance: Lessons from sex myoblast migration in *C. elegans*. *Trends Genet.* **14,** 322–327.

Chin-Sang, I. D., and Chisholm, A. D. (2000). Form of the worm: Genetics of epidermal morphogenesis in *C. elegans*. *Trends Genet.* **16**, 544–551.

Costa, M., Raich, W., Agbunag, C., Leung, B., Hardin, J., and Priess, J. R. (1998). A putative catenin-cadherin system mediates morphogenesis of the *Caenorhabditis elegans* embryo. *J. Cell Biol.* **141,** 297–308.

Fire, A., Harrison, S. W., and Dixon, D. (1990). A modular set of lac-Z fusion vectors for studying gene expression in *C. elegans*. *Gene* **93**, 189–198.

Francis, R., and Waterston, R. H. (1991). Muscle cell attachment in *Caenorhabditis elegans*. *J. Cell Biol.* **114,** 465–479.

George, S. E., Simokat, K., Hardin, J., and Chisholm, A. D. (1998). The VAB-1 Eph receptor tyrosine kinase functions in neural and epithelial morphogenesis in *C. elegans*. *Cell* **92,** 633–643.

Graham, P. L., Johnson, J. J., Wang, S., Sibley, M. H., Gupta, M. C., and Kramer, J. M. (1997). Type IV collagen is detectable in most, but not all, basement membranes of *Caenorhabditis elegans* and assembles on tissues that do not express it. *J. Cell Biol.* **137,** 1171–1183.

Gumbiner, B. M. (1996). Cell adhesion: The molecular basis of tissue architecture and morphogenesis. *Cell* **84,** 345–357.

Hogan, B. L. (1999). Morphogenesis. *Cell* **96,** 225–233.

Horner, M. A., Quintin, S., Domeier, M. E., Kimble, J., Labouesse, M., and Mango, S. E. (1998). *pha-4*, an HNF-3 homologue, specifies pharyngeal organ identity in *Caenorhabditis elegans*. *Genes Dev.* **12,** 1947–1952.

Knust, E. (1997). *Drosophila* morphogenesis: Movements behind the edge. *Curr. Biol.* **7,** R558—R561.

Kuure, S., Vuolteenaho, R., and Vainio, S. (2000). Kidney morphogenesis: Cellular and molecular regulation. *Mech. Dev.* **92,** 31–45.

Labouesse, M. (1997). Deficiency screen based on the monoclonal antibody MH27 to identify genetic loci required for morphogenesis of the *Caenorhabditis elegans* embryo. *Dev. Dyn.* **210,** 19–32.

Labouesse, M., and Mango, S. E. (1999). Patterning the *C. elegans* embryo: Moving beyond the cell lineage. *Trends Genet.* **15,** 307–313.

Legouis, R., Gansmuller, A., Sookhareea, S., Bosher, J. M., Baillie, D. L., and Labouesse, M. (2000). LET-413 is a basolateral protein required for the assembly of adherens junctions in *Caenorhabditis elegans*. *Nat. Cell Biol.* **2,** 415–422.

Leung, B., Hermann, G. J., and Priess, J. R. (1999). Organogenesis of the *Caenorhabditis elegans* intestine. *Dev. Biol.* **216,** 114–134.

Lin, R., Hill, R. J., and Priess, J. R. (1998). POP-1 and anterior-posterior fate decisions in *C. elegans* embryos. *Cell* **92,** 229–239.

Lin, R., Thompson, S., and Priess, J. R. (1995). *pop-1* encodes an HMG box protein required for the specification of a mesoderm precursor in early *C. elegans* embryos. *Cell* **83,** 599–609.

Mango, S. E., Lambie, E. J., and Kimble, J. (1994). The *pha-4* gene is required to generate the pharyngeal primordium of *Caenorhabditis elegans*. *Development* **120,** 3019–3031.

Mello, C. C., Kramer, J. M., Stinchcomb, D., and Ambros, V. (1991). Efficient gene transfer in *C. elegans*: Extrachromosomal maintenance and integration of transforming sequences. *EMBO J.* **10,** 3959–3970.

Mello, C. C., and Fire, A. (1995). DNA transformation. In "*Caenorhabditis elegans*: Modern biological analysis of an organism" (H. F. Epstein and D. C. Shakes, Eds.), pp. 452–482. Academic Press, San Diego.

Metzger, R. J., and Krasnow, M. A. (1999). Genetic control of branching morphogenesis. *Science* **284,** 1635–1639.

Mohler, W. A., Simske, J. S., Williams-Masson, E. M., Hardin, J. D., and White, J. G. (1998). Dynamics and ultrastructure of developmental cell fusions in the *Caenorhabditis elegans* hypodermis. *Curr. Biol.* **8,** 1087–1090.

Nelson, S. H., and McClay, D. R. (1988). Cell polarity in sea urchin embryos: Reorientation of cells occurs quickly in aggregates. *Dev. Biol.* **127,** 235–247.

Newman, A. P., and Sternberg, P. W. (1996). Coordinated morphogenesis of epithelia during development of the *Caenorhabditis elegans* uterine-vulval connection. *Proc. Natl. Acad. Sci. USA* **93,** 9329–9333.

Nodder, S., and Martin, P. (1997). Wound healing in embryos: A review. *Anat. Embryol.* **195,** 215–228.

Pettitt, J., Wood, W. B., and Plasterk, R. H. (1996). *cdh-3*, a gene encoding a member of the cadherin superfamily, functions in epithelial cell morphogenesis in *Caenorhabditis elegans*. *Development* **122,** 4149–4157.

Podbilewicz, B., and White, J. G. (1994). Cell fusions in the developing epithelia of *C. elegans*. *Dev. Biol.* **161,** 408–424.

Pollack, A. L., Runyan, R. B., and Mostov, K. E. (1998). Morphogenetic mechanisms of epithelial tubulogenesis: MDCK cell polarity is transiently rearranged without loss of cell–cell contact during scatter factor/hepatocyte growth factor-induced tubulogenesis. *Dev. Biol.* **204,** 64–79.

Priess, J. R., and Hirsh, D. I. (1986). *Caenorhabditis elegans* morphogenesis: The role of the cytoskeleton in elongation of the embryo. *Dev. Biol.* **117,** 156–173.

Raich, W. B., Agbunag, C., and Hardin, J. (1999). Rapid epithelial-sheet sealing in the *Caenorhabditis elegans* embryo requires cadherin-dependent filopodial priming. *Curr. Biol.* **9,** 1139–1146.

Roubin, R., Naert, K., Popovici, C., Vatcher, G., Coulier, F., Thierry-Mieg, J., Pontarotti, P., Birnbaum, D., Baillie, D., and Thierry-Mieg, D. (1999). *let-756*, a *C. elegans fgf* essential for worm development. *Oncogene* **18,** 6741–6747.

Roy, P. J., Zheng, H., Warren, C. E., and Culotti, J. G. (2000). *mab-20* encodes Semaphorin-2a and is required to prevent ectopic cell contacts during epidermal morphogenesis in *Caenorhabditis elegans*. *Development* **127,** 755–767.

Saxen, L., and Sariola, H. (1987). Early organogenesis of the kidney. *Pediatr. Nephrol.* **1,** 385–392.

Schnabel, R., and Priess, J. (1997). Specification of cell fates in the early embryo. In "*C. elegans* II" (D. L. Riddle, T. Blumenthal, B. J. Meyer, and J. R. Priess, Eds.), pp. 361–382. Cold Spring Harbor Laboratory Press, Cold Spring Harbor, NY.

Sibley, M. H., Graham, P. L., von Mende, N., and Kramer, J. M. (1994). Mutations in the α2(IV) basement membrane collagen gene of *Caenorhabditis elegans* produce phenotypes of differing severities. *EMBO J.* **13,** 3278–3285.

Simske, J. S., and Hardin, J. (2001). Getting into shape: Epidermal morphogenesis in *Caenorhabditis elegans* embryos. *BioEssays.* **23,** 12–23.

Sulston, J. E., Schierenberg, E., White, J. G., and Thomson, J. N. (1983). The embryonic cell lineage of the nematode *Caenorhabditis elegans. Dev. Biol.* **100,** 64–119.

Terns, R. M., Kroll-Conner, P., Zhu, J., Chung, S., and Rothman, J. H. (1997). A deficiency screen for zygotic loci required for establishment and patterning of the epidermis in *Caenorhabditis elegans. Genetics* **146,** 185–206.

White, J. (1988). The anatomy. In "The Nematode *Caenorhabditis elegans* " (W. B. Wood, Ed.), pp. 81–122. Cold Spring Harbor Laboratory Press, Cold Spring Harbor, NY.

Williams, B. D., and Waterston, R. H. (1994). Genes critical for muscle development and function in *Caenorhabditis elegans* identified through lethal mutations. *J. Cell Biol.* **124,** 475–490.

Williams-Masson, E. M., Heid, P. J., Lavin, C. A., and Hardin, J. (1998). The cellular mechanism of epithelial rearrangement during morphogenesis of the Caenorhabditis elegans dorsal hypodermis. *Dev. Biol.* **204,** 263–276.

Williams-Masson, E. M., Malik, A. N., and Hardin, J. (1997). An actin-mediated two-step mechanism is required for ventral enclosure of the *C. elegans* hypodermis. *Development* **124,** 2889–2901.

Wright, K. A., and Thomson, J. N. (1981). The buccal capsule of *Caenorhabditis elegans* (Nematoda: Rhabditoidea): An ultrastructural study. *Can. J. Zool.* **59,** 1952–1961.

Wu, S. L., Staudinger, J., Olson, E. N., and Rubin, C. S. (1998). Structure, expression, and properties of an atypical protein kinase C (PKC3) from *Caenorhabditis elegans*. PKC3 is required for the normal progression of embryogenesis and viability of the organism. *J. Biol. Chem.* **273,** 1130–1143.

Yeaman, C., Grindstaff, K. K., and Nelson, W. J. (1999). New perspectives on mechanisms involved in generating epithelial cell polarity. *Physiol. Rev.* **79,** 73–98.

Zipkin, I. D., Kindt, R. M., and Kenyon, C. J. (1997). Role of a new Rho family member in cell migration and axon guidance in *C. elegans. Cell* **90,** 883–894.

Submitted for publication January 3, 2001
Revised February 15, 2001
Accepted February 16, 2001
Published online April 16, 2001